Biomaterials Science



PAPER View Article Online
View Journal | View Issue



Cite this: *Biomater. Sci.*, 2019, **7**, 3876

Received 4th June 2019, Accepted 2nd July 2019 DOI: 10.1039/c9bm00867e

rsc.li/biomaterials-science

Covalent conjugation of bioactive peptides to graphene oxide for biomedical applications†

Karoline E. Eckhart, Da Brian D. Holt, Da Michaela G. Laurencin Db and Stefanie A. Sydlik D**

Graphene is a valuable material in biomedical implant applications due to its mechanical integrity, long-range order, and conductivity; but graphene must be chemically modified to increase biocompatibility and maximize functionality in the body. Here, we developed a foundational synthetic method for co-valently functionalizing a reduced GO with bioactive molecules, focusing on synthetic peptides that have shown osteogenic or neurogenic capability as a prototypical example. X-ray photoelectron spectroscopy provides evidence that the peptide is covalently linked to the graphenic backbone. These peptide–graphene (Pep–G) conjugate materials can be processed into mechanically robust, three-dimensional constructs. Differences in their electrostatic charges allow the Pep–G conjugates to form self-assembled, layer-by-layer coatings. Further, the Pep–G conjugates are cytocompatible and electrically conductive, leading us to investigate their potential as regenerative scaffolds, as conductive surfaces can stimulate bone and nerve regeneration. Notably, PC12 cells grown on an electrically stimulated Pep–G scaffold demonstrated enhanced adhesion and neurite outgrowth compared to the control. The functionalization strategy developed here can be used to conjugate a wide variety of bioactive molecules to graphene oxide to create cell-instructive surfaces for biomedical scaffold materials.

Introduction

Traumatic injuries often require surgical implants to guide the body towards repair. To best accomplish healing, implant materials must be biocompatible, durable, have similar mechanical properties to the native tissue, and be able to act as a scaffold for cellular growth.⁵ Current implant technologies often lack one or more of these requirements, resulting in inferior healing for the afflicted patient.^{5,6} To address the shortcomings of current implant technologies, researchers are focused on developing new implant materials. Graphene, graphene oxide (GO), and reduced GO (rGO) are materials of interest due to their mechanical strength, conductivity, and long-range order that mimic those of biological tissues.^{7,8} Such graphenic materials intrinsically support cell adhesion,9-11 but biocompatibility can vary depending on particle size and functionalization. 12,13 Thus, researchers have developed ways to functionalize graphene, GO, and rGO with biocompatible moieties such as PEG, dextran, and poly(acrylic acid).14-17 While these surface modifications allow safer

implementation of graphenic materials for medical applications, they are bioinert and do not specifically direct healing.

Recently, a large area of research has focused on creating functional graphenic materials (FGMs) that provide biochemical cues to instruct cells towards healing. 7,18,19 FGMs of this nature can be made by covalently functionalizing GO (or rGO) through its oxygen-containing chemical handles to install bioactive moieties. For example, our group has chemically modified GO to bear hydroxyapatite-mimicking polyphosphate moieties coordinated with calcium cations. In aqueous environments, these materials elute PO₄³⁻ and Ca²⁺ ions that promote osteogenesis in vitro and induce ectopic bone formation in vivo.²⁰ In another example, the bioactive arginylglycylaspartic acid (RGD) peptide was covalently conjugated to GO, resulting in a graphenic material that enhanced adhesion and proliferation of human periodontal ligament fibroblasts.²¹ We aim to expand this area of research by covalently functionalizing a GO derivative with synthetic, bioactive peptides. We theorize that this would give a class of peptide-graphene (Pep-G) conjugate materials that express both the bioactivity of the peptide as well as the favorable material properties of the graphenic component.

Here, we designed Pep-G materials to target osteogenesis and neurogenesis, both of which can be enhanced by scaffold conductivity and peptide identity. Conductive surfaces are

^aDepartment of Chemistry, Carnegie Mellon University, Pittsburgh, PA, USA

^bDepartment of Electrical and Computer Engineering, Carnegie Mellon University, Pittsburgh, PA, USA

[†]Electronic supplementary information (ESI) available. See DOI: 10.1039/c9bm00867e

Biomaterials Science

known to promote cellular adhesion and proliferation,22 and they induce osteogenesis 1-3 and neurogenesis 4 when pulsed with electrical current.¹⁻⁴ As such, we used Claisen graphene (CG)²³ as our parent graphenic scaffold because it is a reduced GO, which not only offers greater conductivity compared to neat GO, but is also more cytocompatible.²⁴ We targeted polyglutamate (p(Glu)) and polylysine (p(Lys)) as our peptide conjugates because p(Glu), especially deprotected p(Glu)₇ ²⁵ and benzyl-protected p(Glu-Bzl),²⁶ promotes osteogenesis, while p(Lys) is known to promote cellular adhesion with its positive charge²⁷ as well as aid differentiation of stem cells into neuronal cells.²⁸

Previously, our group developed a method to synthesize Pep-Gs by grafting peptides from CG through a ring-opening polymerization of α-amino acid N-carboxyanhydride (NCA) monomers from nucleophilic initiating sites on the surface of CG.29 This strategy gave rise to a class of biocompatible and mechanically robust Pep-G materials. While these materials represent promising cell scaffold materials, the synthetic technique is limited. Control over peptide length and molecular weight dispersity is challenging due to difficulty in precisely defining the number of initiating sites on CG. Further, the presence of other non-initiating functional groups and adsorbed water on CG hamper the sensitive NCA polymerization. The ability to precisely define and control the identity of the peptide conjugated to the graphenic surface is critical to harnessing the surface functionality of a biomaterial in vivo.

To address these challenges, this work presents a foundational method for covalently conjugating peptides to CG using a grafting to synthetic strategy. This technique not only allows conjugated peptides to be precisely defined prior to conjugation, but it also enables unprecedented control over peptide molecular weight with molecular weight dispersities as low as 1.11. Characterization via X-ray photoelectron spectroscopy (XPS) provides evidence that the peptides are covalently attached to CG.

In this study, protected homopeptides of polylysine and polyglutamate were conjugated to CG, then deprotected to reveal charged functional groups on the peptide side chains. Our Pep-G conjugates, both protected and deprotected, are cytocompatible and can be processed into mechanically robust 3D constructs or applied as a coating through electrostatic selfassembly. Constructs of the Pep-G materials also show a notable enhancement in conductivity compared to those of the parent graphenic materials (GO and CG), a feature that further constitutes their intrinsic function in the body. In fact, this cell-instructive characteristic was explored in a preliminary nerve regeneration study, which demonstrated that cell adhesion and neuronal-like differentiation was enhanced for PC12 cells that were cultured on an electrically stimulated Pep-G pellet.

This research presents a class of Pep-G materials that have promise as regenerative tissue scaffolds. Moreover, the CG functionalization strategy itself may have major implications in the realm of biomaterials as the synthesis can be tuned to covalently link virtually any bioactive moiety to CG to create FGMs that target a specific healing pathway.

Experimental

Materials

L-Glutamic acid γ-benzyl ester and N₆-carbobenzyloxy-L-lysine were purchased from Chem-Implex International, Inc. and used without further purification. Triphosgene was purchased from TCI America and used without further purification. Hexylamine was purchased from Aldrich. Natural flake graphite (-325 mesh, 99.8% metal basis), trifluoroacetic acid, hydrobromic acid (48% w/w aqueous), and poly(allylamine hydrochloride) were purchased from Alfa Aesar. Glacial acetic acid was purchased from Fisher Chemical. Dry tetrahydrofuran was obtained directly from a dry solvent still. Dioxane and dimethylformamide were dried by passing through a column of activated alumina.

NCA monomer synthesis

Standard literature procedure was used to synthesize γ-benzyl-L-glutamate NCA (Glu(Bzl)-NCA) and ε-benzyloxycarbonyl-Llysine NCA (Lys(Z)-NCA).30

Electrophilic CG (ECG) synthesis

GO was synthesized from graphite using a modified Hummers' method, 31 giving particles with a z-average diameter of approximately 2.4 ± 1.4 µm by dynamic light scattering (DLS) (Fig. S1†). GO was reacted to form a saponified CG (z-average diameter of 2.7 ± 1.2 μm by DLS, Fig. S1†) as previously described by our group.²³ An oven-dried, round bottom flask was charged with CG (0.9 g), dry dioxane (175 mL), and dry dimethylformamide (0.9 mL). The CG was dispersed via sonication (10 min, 240 W, 42 kHz, ultrasonic cleaner, Kendal), then SOCl2 (5.3 mL) was added to the reaction flask, dropwise, while stirring vigorously under a constant flow of N2. After stirring for 15 h at room temperature under N2, the reaction solution was quickly vacuum filtered and rinsed with dichloromethane (under ambient conditions). The resulting filter cake of ECG was immediately used for peptide endcapping.

Peptide synthesis and endcapping

In a typical polymerization, an oven-dried, round bottom flask was charged with NCA monomer and placed under high vacuum overnight. After refilling the flask with N2, the monomer was dissolved in dimethylformamide (2.2 mL mmol⁻¹ monomer). To the stirring monomer solution, the hexylamine initiator was added from a stock solution (in dimethylformamide). After 10 min, the reaction was placed under light vacuum. After 2 days of stirring at room temperature under vacuum, the reaction solution was cut with dichloromethane (2.2 mL mmol⁻¹ NCA monomer), the ECG filter cake was added, and the resulting solution was sonicated for 10 min. ECG was added in a ratio of 0.5 mmol of peptide per gram of CG. After stirring for 2 days, the endcapping reaction solution was vacuum filtered and rinsed several times with dimethylformamide, deionized water, acetone, and di**Paper Biomaterials Science**

chloromethane. The resulting Pep-G materials were dried under vacuum overnight and stored in a desiccator.

Peptide deprotection

Deprotection of unconjugated peptide was performed using a previously reported literature procedure.³² Pep-G conjugates (200 mg) were dispersed in glacial acetic acid (5 mL) via sonication (10 min). Trifluoroacetic acid (2 mL) and 48% aqueous hydrobromic acid (1 mL) were added to the dispersion, and the reaction was stirred at room temperature for 48 h. The resulting reaction solutions were centrifuged at 2160g for 10 min (Z 366, HERMLE Labortechnik GmbH, Wehingen, Germany) and the supernatant discarded. The pellet was washed by resuspension in solvent, centrifugation, and decanting. Wash steps were performed twice with deionized water, once with acetone, and twice with diethyl ether. All supernatants from wash steps were discarded. The deprotected Pep-G pellet was dried under vacuum overnight and stored in a desiccator.

3-D construct fabrication

A stainless steel die of 2.54 cm height, 6.350 cm outer diameter, and 3.749 mm inner diameter and punches of 3.749 mm diameter reference fit to die with 0.020 mm clearance per side were used to create pellets with a diameter of ~3.75 mm. Between 20-25 mg of powder material was added to the room temperature mold, pressed for 1 min with a Columbian D63 $\frac{1}{2}$ bench vise, and removed.

Layer-by-layer coating

CG and p(Lys)_{long}-G dispersions (0.5 mg mL⁻¹ in deionized water) were prepared, and their pH was adjusted to 9 and 4, respectively, using dilute hydrochloric acid and sodium hydroxide solutions. Following a 30-minute plasma treatment, glass slides were soaked for 20 min in a 10 mm solution of cationic poly(allylamine hydrochloride) which had been adjusted to pH 4. Next, the glass slide was alternately dipped for 20 minutes in either anionic (CG) or cationic (p(Lys)_{long}-G) graphenic dispersions; then, without rinsing, the slide was dried under a gentle stream of nitrogen. Ultraviolet-visible spectra of the dry, coated substrate were acquired after the addition of each layer. The slide was coated with a total of 10 graphenic layers.

Cell culture

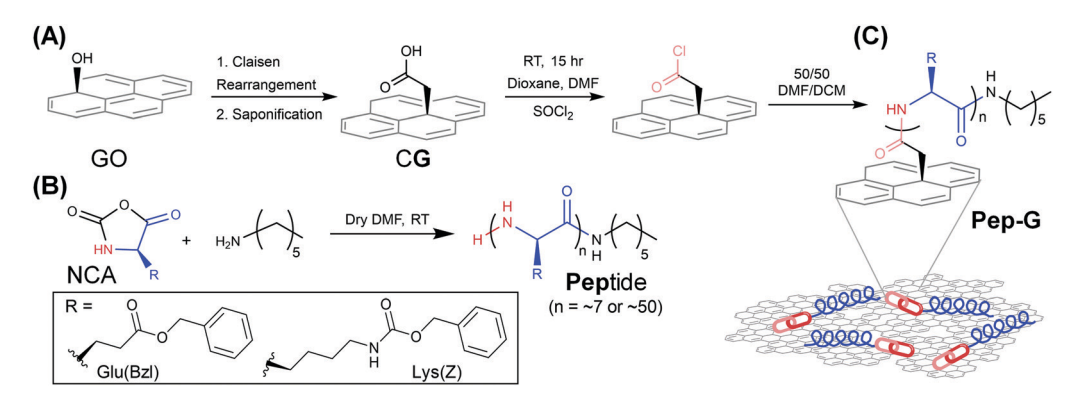
PC12 cells are a cell line that was isolated from a rat pheochromocytoma. PC12 cells were generously provided by Prof. M. Bruchez at Carnegie Mellon University who originally obtained them from American Type Culture Collection (ATCC® CRL-1721TM). For complete cell culture details, see ESI.†

Results and discussion

Synthesis of Pep-G conjugates

To conjugate the graphenic component with the peptide, we aimed to couple through an amide bond, since this type of bond is relatively impervious to hydrolysis unless enzyme catalyzed. An amide linkage can be obtained by reacting the N-terminus of the peptide with activated carboxylic acids on the edges of a GO sheet.33 However, this would result in an amide linkage that is directly attached to the sp² hybridized carbon network of graphene, making the tether bond especially susceptible to hydrolysis due to resonance through the graphenic backbone.34 To circumvent this, our group used a Claisen rearrangement to convert tertiary alcohols on the basal plane of GO into carboxylic acids that are separated from the graphenic surface through an sp³ methylene bond (Scheme 1A).²³ This reaction gives rise to Claisen graphene (CG), a reduced GO with numerous carboxylic acids decorating the graphenic sheet surface and edges. The surface and edge carboxylic acids of CG act as electrophilic chemical handles that can be used to couple nucleophile-terminated peptides.

To increase the electrophilicity of CG and enhance the coupling efficiency, carboxylic acids on CG were transformed into acyl chlorides by reacting them with thionyl chloride (Scheme 1A). Concurrently, protected NCA monomers of Lysine (Z) and Glutamate(Bzl) were polymerized through a controlled



Scheme 1 (A) Graphene oxide (GO) is converted to Claisen graphene (CG), 23 then is modified to bear electrophilic acyl chlorides. (B) NCA monomers are polymerized to give a nucleophilic terminal amine on p(Lys-Z) or p(Glu-Bzl). (C) The electrophilic CG is coupled with nucleophilic peptides to give peptide-graphene (Pep-G) conjugates.

Biomaterials Science Paper

ring-opening polymerization initiated by hexylamine to give peptides with a nucleophilic amine end group (Scheme 1B). Following completion of the NCA polymerizations, the polymerization solutions were quenched with the electrophilic CG to yield protected Pep-G conjugates (Scheme 1C).

We wanted to assess the extent of noncovalent peptide adsorption to CG following the purification protocol. To address this, a control endcapping experiment was designed where a p(Lys-Z) peptide with no nucleophilic end group was subjected to CG endcapping conditions (Fig. S2A†). Following purification (Fig. S2B†), the resultant graphenic material was shown to contain minimal adsorbed peptide (Fig. S2C†), demonstrating the need for complimentary chemical handles on the peptide and CG components of the coupling reaction. Notably, this control experiment also demonstrated the efficacy of the material purification procedure, as much of the unbound peptide was isolated in the reaction supernatant (Fig. S2D†).

Prior to endcapping the polymers with CG, an aliquot of the polymerization solution was reserved for analysis by ¹H NMR and GPC (Fig. S3 and Table S2†). Using a grafting to synthetic strategy allows the bioactive moiety to be both versatile and well-defined.

Long and short protected peptides of p(Glu-Bzl) and p(Lys-Z) were conjugated to CG to yield p(Glu-Bzl)_{long}-G, p(Glu- $Bzl)_{short}$ -G, $p(Lys-Z)_{long}$ -G, and $p(Lys-Z)_{short}$ -G. Different peptide lengths were conjugated to CG to demonstrate the versatility and tunability of this conjugation technique. The protected Pep-G conjugates could then be deprotected in acidic conditions to expose the amine and carboxylic acid side chain of the p(Lys) and p(Glu) peptide, respectively.

Characterization of Pep-G conjugates

The Pep-G conjugates were characterized by Fourier transform infrared spectroscopy (FTIR), thermogravimetric analysis (TGA), and X-ray photoelectron spectroscopy (XPS).

Using FTIR, the existence of peptide in the protected Pep-G conjugates is supported by the presence amide bonds from the backbone of the peptide at 1544 and 1653 cm⁻¹ (Fig. S4†). Peptide conjugation is further reinforced by changes in the thermal degradation profile by TGA (Fig. S5†). Protected Pep-G conjugates show two degradation events between 100 and 400 °C. The first degradation event has an onset temperature $(T_{\rm o})$ of ~140 °C and likely corresponds to the degradation of unreacted carboxylic acids from the graphenic surface.³⁵ The second degradation event has an $T_{\rm o}$ of ~220 °C and likely corresponds to peptide degradation since the neat peptides have an T_0 of ~217 °C and ~220 °C for p(Lys-Z) and p(Glu-Bzl), respectively. Thus, peptide coupling through the carboxylic acids of CG is supported by a decrease in the percent weight loss of the first degradation event (carboxylic acids) compared to CG, and by the strong presence of a second degradation event in the Pep-Gs that corresponds to peptide decomposition.

While FTIR and TGA can be useful tools for demonstrating functionalization of graphenic materials, 17,33,36 these techniques cannot confirm or define covalent attachment of CG to

the peptide, as noncovalent adsorption would produce these same results. XPS, on the other hand, allows more specific characterization of these materials through both atomic survey scans and high resolution atomic scans.

XPS survey scans indicate that the protected Pep-G conjugates contain peptide because these materials exhibit a nonzero percent nitrogen, while the Pep-G synthetic precursors, GO and CG, show a complete lack of nitrogen (Fig. 1A). The nitrogen content in each protected Pep-G was used to quantify the percent of total atoms on the Pep-G surface that could be attributed to peptide (Fig. 1B). This calculation is shown in the ESI (Scheme S1†). The atomic percent peptide metric provides a broad view of the overall functionalization density of the conjugate.

Peak fitting of high resolution XPS is a powerful and commonly used tool when homing in on a specific chemical modification within a complex material. Deconvolution of high resolution N 1s XPS provides evidence that the peptide is covalently attached to CG in the protected Pep-G conjugates. The amine peak (centered at 400.7 eV) represents the end group from which the peptides were coupled to the CG: absence of the amine in N 1s XPS demonstrates conjugation through this functional group. The protected Pep-G conjugates described herein show no amine peak, supporting the contention that the peptides are covalently bound to the CG sheet through their N-terminus (Fig. 1C). On the other hand, noncovalent blends of CG with p(Lys-Z) or p(Glu-Bzl) exhibit small amine peaks, representing the uncoupled N-terminus of the peptide (Fig. 1C).

Deprotection of the Pep-G conjugates was also examined through deconvolution of high resolution XPS spectra. For p(Lys)-G materials, high-resolution N 1s spectra revealed reductions of the carbamate peak (398.4 eV) in the protected materials (50.8 \pm 0.1%) that were equal to the sum of the amine (400.7 eV) and ammonium (402-403 eV) peaks in the deprotected materials (45.4 \pm 6.8%) (Fig. 2A and Fig. S6A†). This result is expected because hydrolysis of the protecting group at the carbamate moiety leaves a primary amine (or ammonium, when protonated) on the side chain of each deprotected lysine residue. The amide peak (399.3 eV) remains virtually the same between the protected and deprotected p(Lys)-Gs because the peptide backbone is unaffected by the deprotection conditions.

Similarly, high-resolution XPS O 1s spectra of p(Glu)-G materials demonstrated successful peptide deprotection. The percent decreases of C-O (530.9 eV) in the protected p(Glu)-Gs (18.2% and 6.6% for long and short peptides, respectively) are approximately equal to the percent increases in -OH (533.6 eV) in the deprotected p(Glu)-Gs (17.4% and 7.7% for long and short peptides, respectively) (Fig. 2B and Fig. S6B†). The C-O functional group can be partially attributed to the benzyl ester protecting group on the protected p(Glu-Bzl)-Gs. When this protecting group is removed, those C-O bonds are quantitatively replaced with -OH bonds, representing the hydroxyl component of the deprotected poly(glutamic acid). Interestingly, -OH bonds are also present in the protected p(Glu-Bzl)-G

Paper Biomaterials Science

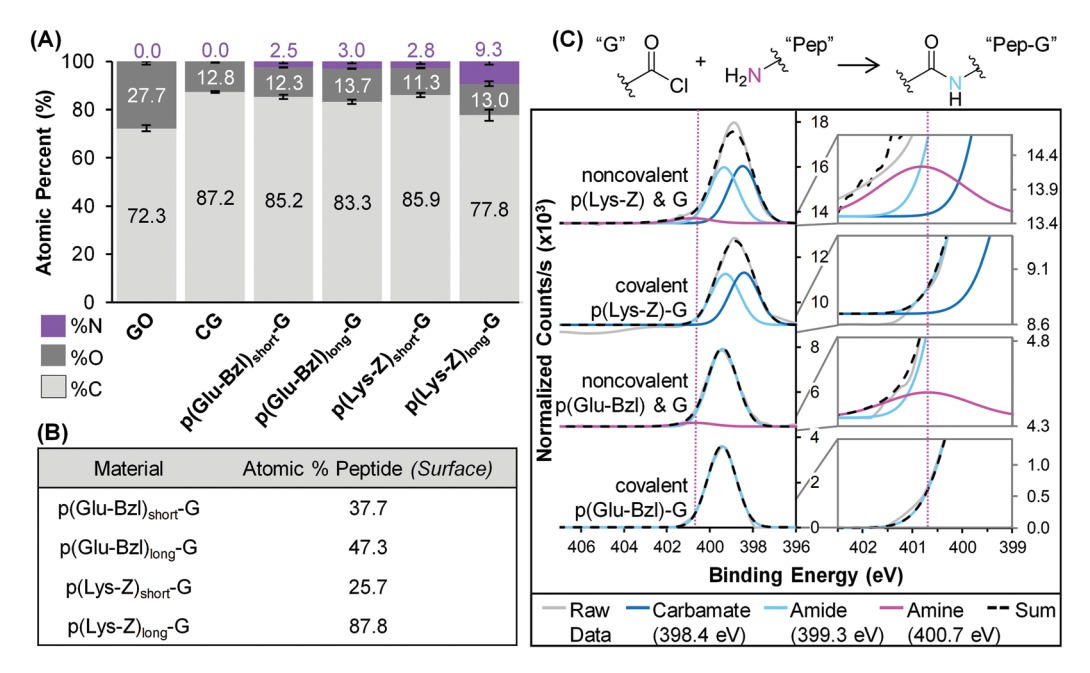


Fig. 1 (A) Presence of nitrogen in XPS survey scans of protected Pep-G conjugates indicates successful peptide conjugation. (B) XPS survey scans can be used to calculate the percent of atoms on the Pep-G surface that can be attributed to the peptide. (C) Covalent peptide attachment is suggested through a comparison of high resolution N 1s XPS spectra of covalent versus noncovalent Pep-G conjugation.

materials, and the experimental change in percent of each functional group represented by the O 1s spectra does not perfectly align with the theoretical change based on the chemical modification. This result is due to other oxygen-containing functional groups present on CG that are not associated with the peptide. The amide (531.6 eV) and carbonate (532.6 eV) peaks remain virtually unchanged between the protected and deprotected p(Glu)–Gs because these groups are not affected by the deprotection conditions.

Assessment of bulk properties

Three dimensional (3D) scaffolds of the Pep–G conjugates and their parent materials (GO and CG) were constructed by pressing the powder material into a cylindrical pellet. The pellets were evaluated for their electrical conductivity, bulk density, and mechanical integrity to assess their potential as 3D implant materials.

Pep–G pellets were found to have excellent conductivity (Fig. 3A). Covalent peptide conjugation to CG, yielding a protected Pep–G, results in a notable increase in conductivity by an order of magnitude over CG (between 0.48 and 0.57 S m $^{-1}$ versus 9.0×10^{-2} S m $^{-1}$). This trend appears to be related to the smaller interlayer spacing of the covalent Pep–Gs compared to CG, as demonstrated by X-ray diffraction (XRD) (Fig. S7†). Interactions such as hydrogen bonding and chain entanglement between peptides that are covalently bound to adjacent Pep–G sheets may cause the peptides to pull CG sheets closer together, facilitating a better conductivity pathway.

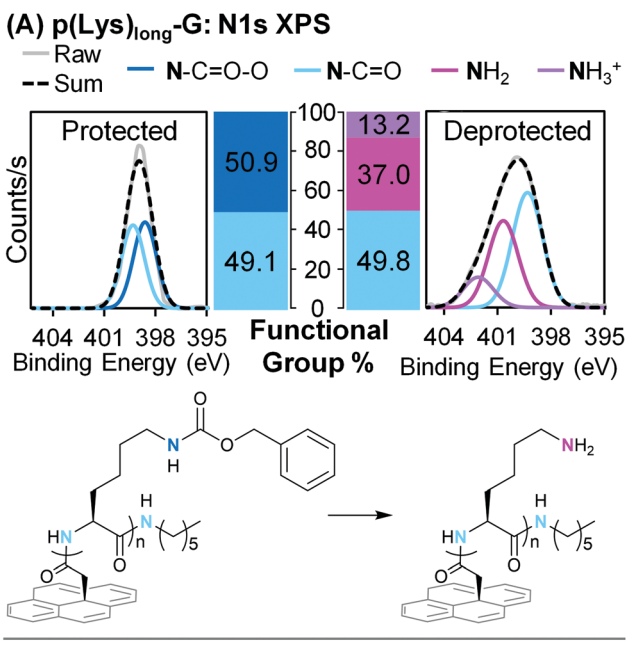
On the other hand, noncovalent blends of p(Glu-Bzl) with CG are less conductive ($6.3 \times 10^{-4} \text{ S m}^{-1}$) than neat CG. This may be explained by phase separation between the peptide

and CG components of the mixture: pockets of insulating peptide may create barriers between CG aggregates, decreasing the conductivity of the pellet by blocking a pathway for electron mobility. Pep–Gs, which are covalently conjugated, do not experience phase separation.

When peptides on the Pep–G are deprotected, conductivity significantly increases compared to when the peptides were protected. Again, XRD demonstrates that the deprotected Pep–Gs have more homogenously small interlayer spacing than the protected Pep–Gs, which correlates to this conductivity trend (Fig. S7†). The elevated conductivity of the deprotected Pep–Gs may also be supplemented by electron mobility through the charged peptide sidechains.

3D constructs of the protected Pep-G materials exhibited mechanical properties similar to those of their parent graphenic materials, GO and CG, and significantly better than those of noncovalent peptide and CG mixtures (Fig. 3B, C and Fig. S8, S9†). Interestingly, deprotection of the peptide within the Pep-G conjugate resulted in a stiffer material, as seen in the consistently enhanced Young's Moduli (E) of the deprotected Pep-Gs compared to their protected counterparts. This property may result from entanglement between deprotected peptides on adjacent Pep-G sheets, which have more entropic freedom^{37,38} than protected peptides, resulting in mechanical stabilization of the bulk material. Again, noncovalent blends of CG with peptide exhibited weakened bulk properties: UCS (0.59 MPa), Young's Modulus (0.047 MPa), and toughness $(2.36 \times 10^{14} \text{ J m}^{-3})$ were two orders of magnitude lower than the covalent Pep-G constructs (Fig. S9†). These results may be indicative of phase separation between the CG and noncovalently blended peptide, leading to mechanical weakening.

Biomaterials Science



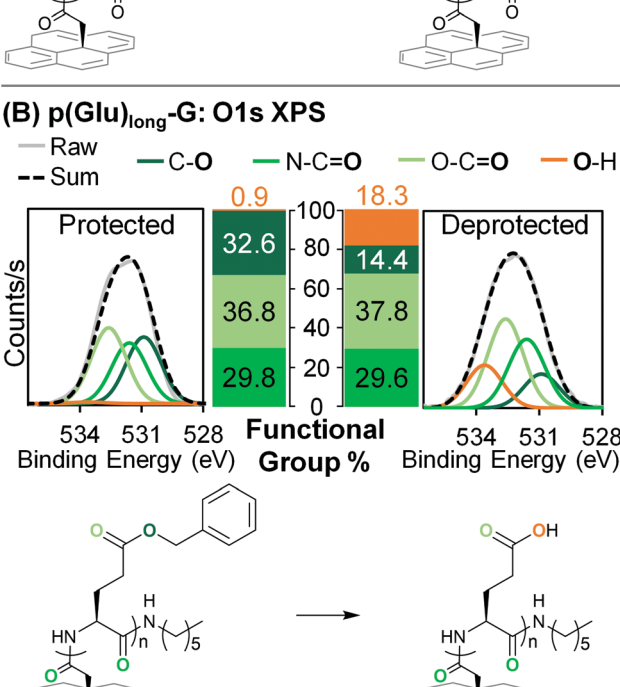


Fig. 2 Deprotection of $p(Lys-Z)_{long}-G$ (A) and $p(Glu-Bzl)_{long}-G$ (B) materials is indicated by deconvolution of N 1s and O 1s XPS spectra, respectively. Percentages of each nitrogen or oxygen-containing functional group within the Pep-G conjugates demonstrate deprotection of peptides. This figure shows representative data from $(Pep)_{long}-G$ materials. Data for conjugates with short peptide can be seen in $(Fig. S6\dagger)$.

The conductivity and mechanical trends observed here demonstrate two main points: (1) the Pep–G materials (both protected and deprotected) have equivalent or enhanced bulk properties when compared to their parent graphenic materials (CG and GO); and (2) *covalent* attachment of the peptide to the CG is critical to retaining or improving the bulk material properties, as noncovalent blends and peptide with CG were both

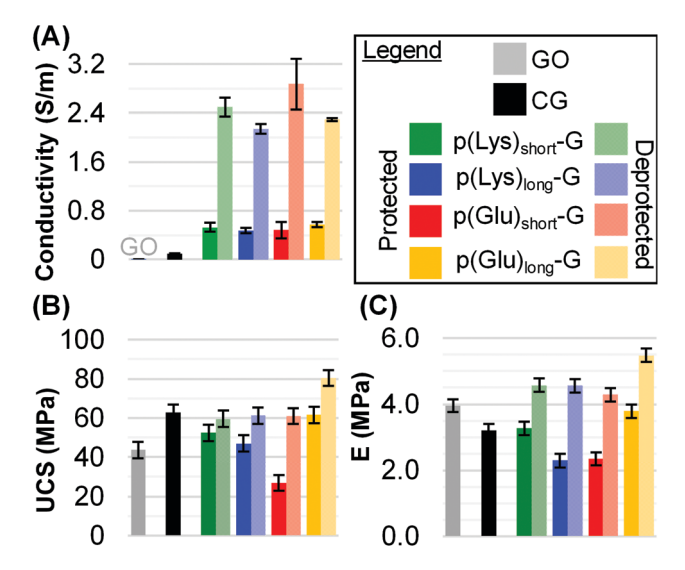


Fig. 3 (A) Pep-G conjugates, particularly with a deprotected peptide, show enhanced conductivity compared to CG and GO. Ultimate compressive strength (B) and Young's Modulus (C) of pressed pellets were calculated from stress-strain curves.

nonconductive and mechanically inferior when compared to covalent Pep-Gs.

Biomedical implant materials should mimic the mechanical properties of the anatomical tissue surrounding the implant.³⁹ Pressing the Pep–G conjugates into 3D pellets, as in this research, results in Young's moduli comparable to muscle tissue; yet, the pellets are not stiff enough for load-bearing applications like bone.⁷ Further research in processing powder graphenic materials into 3D constructs must be done to give tunability to the mechanical stiffness so that these materials can be implemented as surgical implants for wider variety of anatomical tissues. On the other hand, the conductivity of the protected Pep–G materials is similar in magnitude to nerve and skeletal muscle (0.2–0.7 S m⁻¹).⁴⁰ As such, the protected Pep–G materials may be suitable implant materials to surround and regenerate these types of native tissues.

Layer-by-layer coatings

GO and most preparations of reduced GO are inherently negatively charged in solution due to their acidic, oxygen-containing functional groups. This property is evident given the -44.7 and -65.3 mV zeta potentials of GO and CG, respectively (Fig. 4A). The zeta potential of CG is more negative than that of GO because the former has been functionalized with additional carboxylic acids, making the material more acidic in solution. When protected peptides are covalently bound to CG, the zeta potential of the resulting material becomes less negative due to functionalization through the acidic carboxylic acid groups on the CG. Deprotection of the p(Lys)–G conjugates exposes basic primary amines on the peptide sidechains, resulting in varying degrees of positive zeta potential based on the length of the conjugated peptide. Experimentally, deprotected p(Lys)_{short}–G and p(Lys)_{long}–G have zeta potentials of

Paper

(A) 25 0.12 Zeta Potential (mV) 5 GO Absorbance 0.09 -15 0.06 0.03 -35 0 -55 O 2 6 8 10 -75 Layer

Fig. 4 (A) Zeta potentials of Pep-G conjugates (solid bar is protected Pep-G, hatched bar is deprotected Pep-G) compared to GO and CG. (B) Electrostatic layer-by-layer coating of alternating CG^- and $p(Lys)_{long}-G^+$ shows a linear increase in absorbance at 500 nm with the addition of layers.

+3.1 and +20.4 mV, respectively (Fig. 4A). Negatively and positively charged materials have been previously used in concert to construct layer-by-layer coatings by harnessing the electrostatic attractions between the materials.41 This principle can be utilized for the construction of coatings with alternating positive and negatively charged graphenic materials.

Layer-by-layer coatings on glass slides were constructed using alternating layers of p(Lys)_{long}-G and CG since these materials exhibited the most positive and negative zeta potentials, respectively. Ultraviolet-visible spectroscopy measurements of the glass slides were taken between the addition of each layer to confirm casting of each new layer. The increase in absorbance is directly proportional to the number of layers constructed on the substrate, as shown in Fig. 4B.

Layering these Pep-G conjugates as a coating onto a medical implant could be a useful application of these functional materials at the interface between the implant and the body.

Cell compatibility

For use in biomedical applications an FGM must be compatible. To confirm that these materials are cytocompatible, we investigated how cellular vitality and mortality are affected by exposure to Pep-G materials. We studied a range of concentrations of Pep-G materials: the highest concentration (1000 $\mu g \text{ mL}^{-1}$) enables a determination of the phenomenological response, while the lowest studied concentration (10 µg mL⁻¹) represents a more toxicologically relevant concentration that is still high enough to reveal deleterious effects. To encompass a wide range of cellular phenotypes, we studied Pep-G compatibility with hMSCs to represent a multipotent phenotype important in tissue regeneration, murine RAW 264.7 macrophages to represent an important class of immune cell that is also highly phagocytic, and murine NIH-3T3 fibroblasts that represent an important connective tissue cell type that plays an important role in wound healing.

Cellular exposure to Pep-G materials dispersed in cell culture media resulted in cytocompatibilities that are similar to GO (Fig. 5). Deprotection, type of peptide, and peptide length had no effect on the cellular response. With all graphenic materials tested, cellular vitality is dose-dependent. Yet, GO has been previously shown to be acceptably cytocompatible for biological applications, and high doses (>10 μg mL⁻¹) may artificially reduce cellular vitality because cells are inundated by and covered with graphenic materials.42 Thus, the functionalization of GO into these prototypical functional graphenic materials did not alter the cellular response, demonstrating, with regard to cytocompatibility, the general feasibility of biomedical applications with appropriate materials preparations.

Electrical stimulation of stem cells on Pep-G Scaffold

PAH+

• CG-

p(Lvs)-G⁺

We aimed to perform a proof-of-concept neural tissue engineering study with a pellet of deprotected p(Lys)long-G, as this Pep-G is bioactive, 43 conductive, providing a suitable substrate for electrical stimulation, and positively charged at physiological pH, which is and known to enhance cell adhesion.²⁷ In this study, PC12 cells were seeded onto the surface of a p(Lys)_{long}-G (positive control) and a CG (negative control) pellet and given electrical stimulation.

To provide electrical stimulation cues to the pellets, we designed a circuit to provide pulsed, DC stimulation at the physiologically relevant levels44 of ~1 mV mm-1 and $\sim 1000 \text{ mA cm}^{-2}$ (Fig. S10A-C†). To ensure proper application of electrical stimulation to cells, 45 we designed a cell testing chamber to isolate the cell culture media from the electrical stimulation (Fig. S10D and E†). We used PC12 cells since they are an immortalized cell line from the rat adrenal medulla that differentiate into neuron-like cells with stimulation.46

PC12 cells cultured on an electrically stimulated p(Lys)_{long}-G pellet showed excellent compatibility; and after only two days, cells began to show neurite outgrowths (Fig. 6). Conversely, when PC12 cells were cultured on an electrically stimulated CG pellet, which is non-bioactive and ~24 times less conductive than p(Lys)long-G, there were far fewer cells present and no neurite outgrowths were observed. Although this result is a first-step, proof-of-concept, it is highly exciting; and we plan to further develop our materials and methods in future work to probe the bioactivity and address the potential

Biomaterials Science Paper

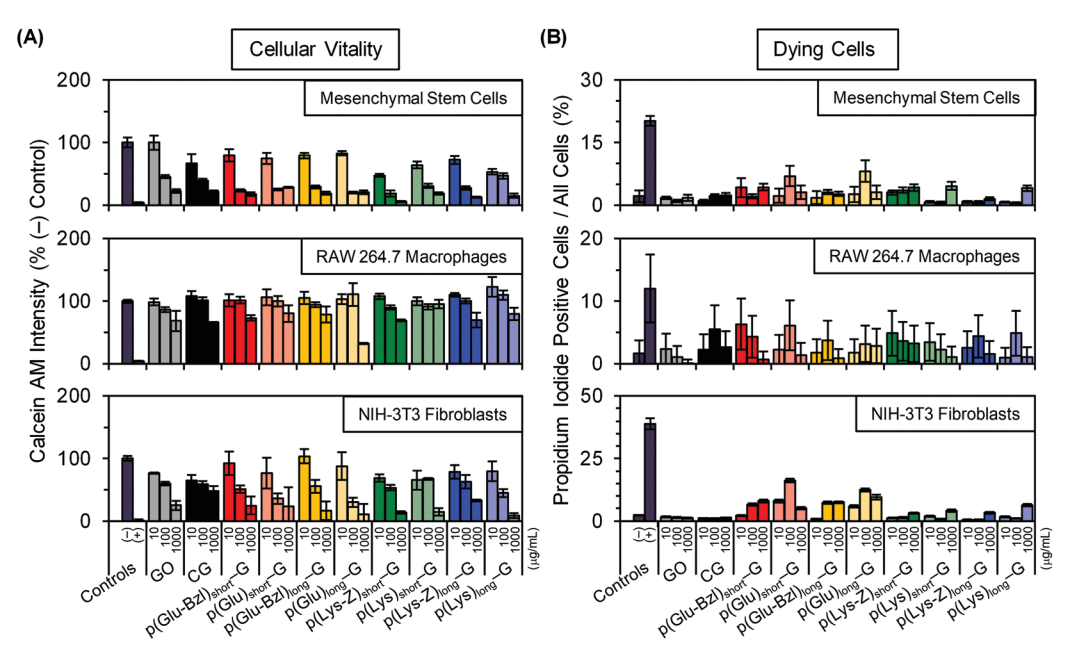


Fig. 5 Cellular vitality (A) and percent dying cells (B) for cells cultured with Pep-G materials is shown in three different cell lines. Pep-G materials are shown to be as cytocompatible as GO, which is commonly accepted as a biocompatible material.

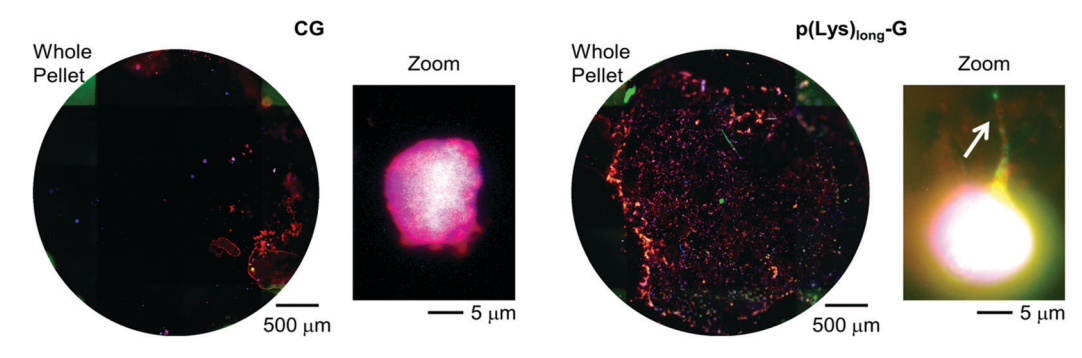


Fig. 6 Overlays of fluorescence images of PC12 cells cultured on electrically stimulated pellets for 2 days. There were a substantial amount of PC12 cells on pellets of p(Lys)_{long}-G, as well as the presence of neurite outgrowths. The bioactivity, electrical conductivity, and interfacial properties of p(Lys)_{long}-G likely enhance the cellular response compared to cells cultured on control pellets of CG. Blue represents DNA; green represents F-actin; red represents mitochondria; and the black circle of the whole pellet images corresponds to the entire surface of the pellet.

of these Pep-G conjugate materials as regenerative tissue scaffolds.

Conclusion and perspective

The GO functionalization technique reported herein enables synthesis of conductive and biocompatible Pep-G conjugates that can be processed into mechanically robust, three-dimensional constructs or electrostatically assembled, layer-by-layer coatings. The conductivity and bioactivity of these Pep-G materials can be harnessed to instruct stem cell differentiation, as PC12 cells grown on an electrically stimulated p(Lys)_{long}-G pellet were shown to have enhanced adhesion and neurite outgrown compared the CG pellet control. This paper also presents a unique characterization strategy through high resolution XPS that provides evidence of covalent peptide conjugation to CG.

Using the functionalization method reported in this paper, this work can be expanded to covalently conjugate CG to other bioactive molecules and biopolymers with nucleophilic chemical handles to give conjugate materials with the functionality of the biomolecule component as well as the favorable mechanical and conductive properties of the graphenic component. If applied as a medical implant, these cell-instructive materials have the potential to facilitate and significantly accelerate healing through regenerative tissue engineering.

Conflicts of interest

There are no conflicts to declare.

Acknowledgements

The authors acknowledge use of the XRD in the Materials Characterization Facility at Carnegie Mellon University under grant # MCF-677785. For providing use of their facilities, we thank R. Gil (NMR, funded in part by NSF grant # CHE-0130903, CHE-1039870, and CHE-1726525), M. Bruchez (microplate reader and PC12 cells), K. Whitehead (NIH-3T3 and RAW 264.7 cells), T. Kowalewski (four-point probe), and K. Matyjaszewski (GPC, light scattering), all at Carnegie Mellon University. We thank J. Gillespie at the University of Pittsburgh for XPS training and use of XPS facilities. We acknowledge Wai Sing Ching for assistance with the design and assembly of the circuit used in the electrical stimulation study. Further, the authors thank Z. Wright for her help with the organization and writing of this paper.

References

- 1 W.-W. Hu, Y.-T. Hsu, Y.-C. Cheng, C. Li, R.-C. Ruaan, C.-C. Chien, C.-A. Chung and C.-W. Tsao, Electrical Stimulation to Promote Osteogenesis Using Conductive Polypyrrole Films, Mater. Sci. Eng., C, 2014, 37, 28-36, DOI: 10.1016/j.msec.2013.12.019.
- 2 C. Li, Y.-T. Hsu and W.-W. Hu, The Regulation of Osteogenesis Using Electroactive Polypyrrole Polymers, 2016, 8(7), 258, DOI: 10.3390/polym8070258.
- 3 J. Cao, Y. Man and L. Li, Electrical Stimuli Improve Osteogenic Differentiation Mediated by Aniline Pentamer and PLGA Nanocomposites, Biomed. Rep., 2013, 1(3), 428-432, DOI: 10.3892/br.2013.70.
- 4 S. Song and P. M. George, Conductive Polymer Scaffolds to Improve Neural Recovery, Neural Regener. Res., 2017, 12(12), 1976-1978, DOI: 10.4103/1673-5374.221151.
- 5 M. Saini, Y. Singh, P. Arora, V. Arora and K. Jain, Implant Biomaterials: A Comprehensive Review, World J. Clin. Cases, 2015, 3(1), 52-57, DOI: 10.12998/wjcc.v3.i1.52.
- 6 A. J. T. Teo, A. Mishra, I. Park, Y.-J. Kim, W.-T. Park and Y.-J. Yoon, Polymeric Biomaterials for Medical Implants and Devices, ACS Biomater. Sci. Eng., 2016, 2(4), 454-472, DOI: 10.1021/acsbiomaterials.5b00429.
- 7 Z. M. Wright, A. M. Arnold, B. D. Holt, K. E. Eckhart and S. A. Sydlik, Functional Graphenic Materials, Graphene Oxide, and Graphene as Scaffolds for Bone Regeneration, Regen. Eng. Transl. Med., 2019, 5(2), 190-209, DOI: 10.1007/ s40883-018-0081-z.
- 8 F. Menaa, A. Abdelghani and B. Menaa, Graphene Nanomaterials as Biocompatible and Conductive Scaffolds for Stem Cells: Impact for Tissue Engineering and Regenerative Medicine, J. Tissue Eng. Regener. Med., 2015, **9**(12), 1321–1338, DOI: 10.1002/term.1910.
- 9 M. Kalbacova, A. Broz, J. Kong and M. Kalbac, Graphene Substrates Promote Adherence of Human Osteoblasts and Mesenchymal Stromal Cells, Carbon, 2010, 48(15), 4323-4329, DOI: 10.1016/j.carbon.2010.07.045.

- 10 S.-R. Ryoo, Y.-K. Kim, M.-H. Kim and D.-H. Min, Behaviors of NIH-3T3 Fibroblasts on Graphene/Carbon Nanotubes: Proliferation, Focal Adhesion, and Gene Transfection Studies, ACS Nano, 2010, 4(11), 6587–6598, DOI: 10.1021/ nn1018279.
- 11 M. Yang, J. Yao and Y. Duan, Graphene and Its Derivatives for Cell Biotechnology, Analyst, 2012, 138(1), 72-86, DOI: 10.1039/C2AN35744E.
- 12 M. Ema, M. Gamo and K. Honda, A Review of Toxicity Studies on Graphene-Based Nanomaterials in Laboratory Animals, Regul. Toxicol. Pharmacol., 2017, 85, 7-24, DOI: 10.1016/j.vrtph.2017.01.011.
- 13 X. Guo and N. Mei, Assessment of the Toxic Potential of Graphene Family Nanomaterials, J. Food Drug Anal., 2014, 22(1), 105-115, DOI: 10.1016/j.jfda.2014.01.009.
- 14 M. Xu, J. Zhu, F. Wang, Y. Xiong, Y. Wu, Q. Wang, J. Weng, Z. Zhang, W. Chen and S. Liu, Improved In Vitro and In Vivo Biocompatibility of Graphene Oxide through Surface Acid)-Functionalization Modification: Poly(Acrylic Superior to PEGylation, ACS Nano, 2016, 10(3), 3267-3281, DOI: 10.1021/acsnano.6b00539.
- 15 W. Miao, G. Shim, S. Lee, S. Lee, Y. S. Choe and Y.-K. Oh, Safety and Tumor Tissue Accumulation of Pegylated Oxide Nanosheets for Co-Delivery Anticancer Drug and Photosensitizer, Biomaterials, 2013, 34(13), 3402-3410, DOI: 10.1016/j.biomaterials.2013.01.
- 16 K. Yang, J. Wan, S. Zhang, Y. Zhang, S.-T. Lee and Z. Liu, In Vivo Pharmacokinetics, Long-Term Biodistribution, and Toxicology of PEGylated Graphene in Mice, ACS Nano, 2010, 5(1), 516-522, DOI: 10.1021/nn1024303.
- 17 S. Zhang, K. Yang, L. Feng and Z. Liu, In Vitro and in Vivo Behaviors of Dextran Functionalized Graphene, Carbon, 2011, 49(12), 4040-4049, DOI: 10.1016/j.carbon.2011.05.056.
- 18 S. R. Shin, Y.-C. Li, H. Jang, P. Khoshakhlagh, M. Akbari, Nasajpour, Y. S. Zhang, A. Tamayol A. Khademhosseini, Graphene-Based Materials for Tissue Engineering, Adv. Drug Delivery Rev., 2016, 105(Pt B), 255-274, DOI: 10.1016/j.addr.2016.03.007.
- 19 X. Ding, H. Liu and Y. Fan, Graphene-Based Materials in Regenerative Medicine, Adv. Healthcare Mater., 2015, 4(10), 1451-1468, DOI: 10.1002/adhm.201500203.
- 20 A. M. Arnold, B. D. Holt, L. Daneshmandi, C. T. Laurencin and S. A. Sydlik, Phosphate Graphene as an Intrinsically Osteoinductive Scaffold for Stem Cell-Driven Bone Regeneration, Proc. Natl. Acad. Sci. U. S. A., 2019, 116(11), 4855-4860, DOI: 10.1073/pnas.1815434116.
- 21 J. Li, L. Zheng, L. Zeng, Y. Zhang, L. Jiang and J. Song, RGD PeptideGrafted Graphene Oxide as a New Biomimetic Nanointerface for Impedance-Monitoring Cell Behaviors, J. Nanomater., 2016, 2016, 2828512, DOI: 10.1155/2016/ 2828512.
- 22 N. A. Habis, K. Lafdi, P. A. Tsonis and K. D. Rio-Tsonis, Enhancing the Cell Growth Using Conductive Scaffolds, J. Nanomed. Nanotechnol., 2018, 9(2), 1-6, DOI: 10.4172/2157-7439.1000493.

23 S. A. Sydlik and T. M. Swager, Functional Graphenic Materials Via a Johnson–Claisen Rearrangement, *Adv. Funct. Mater.*, 2013, 23(15), 1873–1882, DOI: 10.1002/adfm.201201954.

Biomaterials Science

- 24 S. A. Sydlik, S. Jhunjhunwala, M. J. Webber, D. G. Anderson and R. Langer, In Vivo Compatibility of Graphene Oxide with Differing Oxidation States, *ACS Nano*, 2015, 9(4), 3866–3874, DOI: 10.1021/acsnano.5b01290.
- 25 J. L. Bain, B. K. Culpepper, M. S. Reddy and S. L. Bellis, Comparing Variable-Length Polyglutamate Domains to Anchor an Osteoinductive Collagen-Mimetic Peptide to Diverse Bone Grafting Materials, *Int. J. Oral Maxillofac. Implants*, 2014, 29(6), 1437–1445.
- 26 C. Gentilini, Y. Dong, J. R. May, S. Goldoni, D. E. Clarke, B.-H. Lee, E. T. Pashuck and M. M. Stevens, Functionalized Poly(γ-Glutamic Acid) Fibrous Scaffolds for Tissue Engineering, Adv. Healthcare Mater., 2012, 1(3), 308–315, DOI: 10.1002/adhm.201200036.
- 27 D. Mazia, Adhesion of Cells to Surfaces Coated with Polylysine. Applications to Electron Microscopy, *J. Cell Biol.*, 1975, **66**(1), 198–200, DOI: 10.1083/jcb.66.1.198.
- 28 K. E. Crompton, J. D. Goud, R. V. Bellamkonda, T. R. Gengenbach, D. I. Finkelstein, M. K. Horne and J. S. Forsythe, Polylysine-Functionalised Thermoresponsive Chitosan Hydrogel for Neural Tissue Engineering, *Biomaterials*, 2007, 28(3), 441–449, DOI: 10.1016/j. biomaterials.2006.08.044.
- 29 B. D. Holt, A. M. Arnold and S. A. Sydlik, Peptide-Functionalized Reduced Graphene Oxide as a Bioactive Mechanically Robust Tissue Regeneration Scaffold, *Polym. Int.*, 2017, 66(8), 1190–1198, DOI: 10.1002/pi.5375.
- 30 W. H. Daly and D. Poché, The Preparation of N-Carboxyanhydrides of α-Amino Acids Using Bis (Trichloromethyl)Carbonate, *Tetrahedron Lett.*, 1988, 29(46), 5859–5862, DOI: 10.1016/S0040-4039(00)82209-1.
- 31 W. S. Hummers and R. E. Offeman, Preparation of Graphitic Oxide, *J. Am. Chem. Soc.*, 1958, **80**(6), 1339.
- 32 Y. Wang and J. Ling, Synthetic Protocols toward Polypeptide Conjugates via Chain End Functionalization after RAFT Polymerization, *RSC Adv.*, 2015, 5(24), 18546–18553, DOI: 10.1039/C4RA17094F.
- 33 R. Kanchanapally, B. P. V. Nellore, S. Sekhar Sinha, F. Pedraza, S. J. Jones, A. Pramanik, S. Reddy Chavva, C. Tchounwou, Y. Shi, A. Vangara, et al., Antimicrobial Peptide-Conjugated Graphene Oxide Membrane for Efficient Removal and Effective Killing of Multiple Drug Resistant Bacteria, RSC Adv., 2015, 5(24), 18881–18887, DOI: 10.1039/C5RA01321F.
- 34 C. G. Evans and J. D. R. Thomas, Effect of Unsaturated Substituents on the Hydrolysis of Esters, *J. Chem. Soc. B*, 1971, 1502, DOI: 10.1039/j29710001502.

- 35 S. Mallakpour, A. Abdolmaleki and S. Borandeh, Covalently Functionalized Graphene Sheets with Biocompatible Natural Amino Acids, *Appl. Surf. Sci.*, 2014, **307**, 533–542, DOI: 10.1016/j.apsusc.2014.04.070.
- 36 L. Fan, H. Ge, S. Zou, Y. Xiao, H. Wen, Y. Li, H. Feng and M. Nie, Sodium Alginate Conjugated Graphene Oxide as a New Carrier for Drug Delivery System, *Int. J. Biol. Macromol.*, 2016, **93**, 582–590, DOI: 10.1016/j. ijbiomac.2016.09.026.
- 37 D. Huesmann, A. Birke, K. Klinker, S. Türk, H. J. Räder and M. Barz, Revisiting Secondary Structures in NCA Polymerization: Influences on the Analysis of Protected Polylysines, *Macromolecules*, 2014, 47(3), 928–936, DOI: 10.1021/ma5000392.
- 38 M. L. Tiffany and S. Krimm, Circular Dichroism of the "Random" Polypeptide Chain, *Biopolymers*, 1969, **8**(3), 347–359, DOI: 10.1002/bip.1969.360080306.
- 39 F. J. O'Brien, Biomaterials & Scaffolds for Tissue Engineering, *Mater. Today*, 2011, 14(3), 88–95, DOI: 10.1016/S1369-7021(11)70058-X.
- 40 The Biomedical Engineering Handbook: Second Edition, ed. Bronzino, J., CRC Press, Boca Raton, FL, 2nd edn, 1999, vol. 1. DOI: 10.1201/9781420049510.
- 41 Y. He, C. Hong, J. Li, M. T. Howard, Y. Li, M. E. Turvey, D. S. S. M. Uppu, J. R. Martin, K. Zhang, D. J. Irvine, *et al.*, Synthetic Charge-Invertible Polymer for Rapid and Complete Implantation of Layer-by-Layer Microneedle Drug Films for Enhanced Transdermal Vaccination, *ACS Nano*, 2018, 12(10), 10272–10280, DOI: 10.1021/acsnano.8b05373.
- 42 Z. Wright, A. Arnold, B. Holt, K. Eckhart and S. Sydlik, Functional Graphenic Materials, Graphene Oxide, and Graphene as Scaffolds for Bone Regeneration, *Regen. Eng. Transl. Med.*, 2018, 1–20.
- 43 L. Cai, J. Lu, V. Sheen and S. Wang, Promoting Nerve Cell Functions on Hydrogels Grafted with Poly(l-Lysine), *Biomacromolecules*, 2012, 13(2), 342–349, DOI: 10.1021/bm201763n.
- 44 C. D. McCaig, A. M. Rajnicek, B. Song and M. Zhao, Controlling Cell Behavior Electrically: Current Views and Future Potential, *Physiol. Rev.*, 2005, **85**(3), 943–978.
- 45 B. Song, Y. Gu, J. Pu, B. Reid, Z. Zhao and M. Zhao, Application of Direct Current Electric Fields to Cells and Tissues in Vitro and Modulation of Wound Electric Field in Vivo, *Nat. Protoc.*, 2007, 2(6), 1479.
- 46 L. A. Greene, J. M. Aletta, A. Rukenstein and S. H. Green, [18] PC12 Pheochromocytoma Cells: Culture, Nerve Growth Factor Treatment, and Experimental Exploitation, in Methods in Enzymology, Elsevier, 1987, vol. 147, pp. 207–216. DOI: 10.1016/0076-6879(87)47111-5.